Protein-protein contact between the COOH-terminal region of the α subunit and activator proteins may be a widely used mechanism for transcription activation in prokaryotes (*21*). Protein-protein contact between the σ subunit and activator proteins appears to be a second widely used mechanism (*22*). The approach used here should be generalizable to analysis of other prokaryotic and eukaryotic transcription complexes.

REFERENCES AND NOTES

1. S. C. Schultz, G. C. Shields, T. A. Steitz, *Science* **253**, 1001 (1991).
2. A. Kolb, S. Busby, H. Buc, S. Garges, S. Adhya, *Annu. Rev. Biochem.* **62**, 749 (1993).
3. A. Bell *et al.*, *Nucleic Acids Res.* **18**, 7243 (1990); A. Eschenlauer and W. Reznikoff, *J. Bacteriol.* **173**, 5024 (1991); Y. Zhou, X. Zhang, R. Ebright, *Proc. Natl. Acad. Sci. U.S.A.* **90**, 6081 (1993); Y. Zhou, S. Busby, R. Ebright, *Cell* **73**, 375 (1993); T. Heyduk *et al.*, *Nature* **364**, 548 (1993); R. Ebright, *Mol. Microbiol.* **8**, 797 (1993).
4. K. Igarashi and A. Ishihama, *Cell* **65**, 1015 (1991); C. Zou, N. Fujita, K. Igarashi, A. Ishihama, *Mol. Microbiol.* **6**, 2599 (1992); A. Kolb *et al.*, *Nucleic Acids Res.* **21**, 319 (1993); H. Tang, K. Severinov, A. Goldfarb, R. Ebright, in preparation.
5. X. Zhang, Y. Zhou, Y. Ebright, R. Ebright, *J. Biol. Chem.* **267**, 8136 (1992).
6. W. Niu, Q. Dong, Y. Ebright, R. Ebright, in preparation; Y. Zhou and R. Ebright, in preparation.
7. Plasmids pXZCRP (*5*), pXZCRP178S (*8*), and pXZCRP161C;178S encode, respectively, CAP, [Ser^{178}]CAP, and [Cys^{161};Ser^{178}]CAP. Plasmid pXZCRP161C;178S was constructed from plasmid pXZCRP178S by site-directed mutagenesis (*9*). CAP, [Ser^{178}]CAP, and [Cys^{161};Ser^{178}]CAP were prepared as described in (*8*) and were purified from trace contaminating RNAP by centrifugal ultrafiltration at 2000*g* for 8 min at 4°C with the use of 100,000 NMWL polysulfone Ultrafree-MC filter units (Millipore).
8. X. Zhang, A. Gunasekera, Y. Ebright, R. Ebright, *J. Biomol. Struct. Dyn.* **9**, 463 (1991).
9. T. Kunkel, K. Bebenek, J. McClary, *Methods Enzymol.* **204**, 125 (1991).
10. Reaction mixtures (120 μl) contained 125 μM *S*-[*N*-(4-azidosalicyl)cysteaminyl]-2-thiopyridine (Fig. 3A), 124 μM ^{125}I-KI [12.4 becquerels (Bq) per femtomole], 90 mM sodium borate (pH 8.4), and 0.4% dimethyl sulfoxide. Reactions were initiated by transfer to a vial containing 120 nmol 1,3,4,6-tetrachloro-3α,6α-diphenylglycoluril (*11*) [IODO-GEN (Pierce); plated onto the vial walls by evaporation of a 1.2 mM solution in chloroform]. Reactions were terminated after 30 s at 22°C by transfer to a vial containing 15 μl of 8 mM methionine and 1 mM tyrosine. All operations in this and subsequent steps were performed in darkness or under safe-lamp illumination.
11. P. Fraker and J. Speck, *Biochem. Biophys. Res. Commun.* **80**, 849 (1978).
12. Reaction mixtures (100 μl) contained 4 μM [Cys^{161};Ser^{178}]CAP (*7*), 70 μM [^{125}I]-{*S*[*N*-(3-iodo-4-azidosalicyl)cysteaminyl]-2-thiopyridine} (radioiodinated immediately before use) (Fig. 3, A and B), 50 mM sodium borate (pH 8.3), 8 mM tris-HCl (pH 8.3), 80 mM KCl, 0.4 mM EDTA, 5 mM methionine, 0.6 mM tyrosine, 2% glycerol, and 0.2% dimethyl sulfoxide. Reactions were carried out for 20 min at 22°C. IAC^{161}CAP was purified by chromatography on Bio-Gel P6DG (Bio-Rad) and was stored at −70°C in 40 mM tris-HCl (pH 8.0), 100 mM KCl, 10 mM $MgCl_2$, and 5% glycerol.
13. Quantitation of ^{125}I indicated that the reaction was 100% complete: 1.0 mol of [^{125}I]-[*N*-(3-iodo-4-azidosalicyl)cysteaminyl] was incorporated per mole of [Cys^{161};Ser^{178}]CAP subunit. Control experiments with [Ser^{178}]CAP (*7, 8*) indicated that the reaction was 100% site-specific: <0.01 mol of [^{125}I]-[*N*-(3-iodo-4-azidosalicyl)cysteaminyl] was incorporated per mole of [Ser^{178}]CAP.
14. Abortive initiation in vitro transcription experiments were done as described in (*5*). Reaction mixtures (20 μl) contained 5 nM *lacP(ICAP)* DNA fragment [base pair −121 to +102; prepared by polymerase chain reaction amplification of M13mp2-ICAP replicative-form DNA (*5*)], 40 nM RNAP [prepared as in (*15*); desalted into assay buffer (by Bio-Gel P6DG chromatography) immediately before use], 0 to 40 nM IAC^{161}CAP or CAP, 0.2 mM cAMP, 15 μM [α-^{32}P]UTP (0.3 Bq/fmol), 0.6 μM ApA, 40 mM tris-HCl (pH 8.0), 100 mM KCl, 10 mM $MgCl_2$, and 5% glycerol.
15. D. Hager, D. J. Jin, R. Burgess, *Biochemistry* **29**, 7890 (1990).
16. IAC^{161}CAP and CAP showed identical concentration dependences for stimulation of open-complex formation (half-maximal stimulation at 5 nM; saturation at ≈10 nM). At saturating concentrations, IAC^{161}CAP and CAP stimulated open-complex formation 7-fold and 10-fold, respectively.
17. Reaction mixtures (800 μl) contained 5 nM *lacP-(ICAP)* DNA fragment (*14*), 40 nM RNAP (*14*), 10 nM IAC^{161}CAP, 0.2 mM cAMP, 40 mM tris-HCl (pH 8.0), 100 mM KCl, 10 mM $MgCl_2$, and 5% glycerol. Reaction vessels were polystyrene microcentrifuge tubes held inside borosilicate glass culture tubes (13 mm by 100 mm); these reaction vessels exclude wavelengths <290 nm. Reaction mixtures were incubated for 15 min at 37°C. Reaction mixtures then were UV-irradiated for 20 s at 37°C (350 nm; 1×10^5 erg mm^{-2} s^{-2}) in a Rayonet RPR100 photochemical reactor (Southern New England Ultraviolet). After UV irradiation, 6 mg of solid iodoacetamide was added, samples were incubated for 15 min at 22°C, and samples were concentrated to 20 μl by centrifugal ultrafiltration at 2000*g* for 7 min at 22°C with the use of 30,000 NMWL regenerated-cellulose Ultrafree-MC filter units (Millipore). After concentration, 20 μl of 80 mM iodoacetamide and 15 M urea were added, and samples were incubated for 15 min at 22°C. Aliquots (20 μl) were mixed with 5 μl of 0.5 M tris-HCl (pH 6.8), 50% glycerol, 10% SDS, and 0.1 mg/ml bromophenol blue (Fig. 4A) or with 5 μl of the same solution plus 10% β-mercaptoethanol (Fig. 4B) and were analyzed by SDS–polyacrylamide gel electrophoresis (PAGE) [0.1% SDS, 5 to 15% polyacrylamide gradient gels (Bio-Rad)] followed by autoradiography.
18. Crosslinking and nonreducing SDS-PAGE were done as in (*17*). After electrophoresis, the gel slice corresponding to crosslinked CAP-α was excised, washed, and reacted with hydroxylamine as described (*20*). The gel slice then was equilibrated in 500 μl of 100 mM tris-HCl (pH 6.8), 2% SDS, and 2% β-mercaptoethanol for 30 min at 37°C and analyzed by SDS-PAGE (0.1% SDS, 14% polyacrylamide) followed by autoradiography.
19. Y. Ovchinnikov, V. Lipkin, N. Modyanov, O. Chertov, Y. Smirnov, *FEBS Lett.* **76**, 108 (1977).
20. C. Saris, J. van Eenbergen, B. Jenks, H. Bloemers, *Anal. Biochem.* **132**, 54 (1983).
21. F. Russo and T. Silhavy, *J. Biol. Chem.* **267**, 14515 (1992); A. Ishihama, *J. Bacteriol.* **175**, 2483 (1992).
22. J. Hu and C. Gross, *Mol. Gen. Genet.* **199**, 7 (1985); M. Li, H. Moyle, M. M. Susskind, *Science* **263**, 75 (1994); Kumar *et al.*, *J. Mol. Biol.* **235**, 405 (1994).

23. Supported by NIH grant GM41376 to R.H.E.

23 February 1994; accepted 6 May 1994

Mediation of Epstein-Barr Virus EBNA2 Transactivation by Recombination Signal–Binding Protein J_κ

Thomas Henkel, Paul D. Ling, S. Diane Hayward, Michael Gregory Peterson*

The Epstein-Barr virus (EBV) transactivator protein, termed Epstein-Barr virus nuclear antigen 2 (EBNA2), plays a critical role in the regulation of latent viral transcription and in the immortalization of EBV-infected B cells. Unlike most transcription factors, EBNA2 does not bind directly to its cis-responsive DNA element but requires a cellular factor, termed C-promoter binding factor 1 (CBF1). Here, CBF1 was purified and was found to directly interact with EBNA2. CBF1 is identical to a protein thought to be involved in immunoglobulin gene rearrangement, RBPJ$_\kappa$. Contrary to previous reports, CBF1-RBPJ$_\kappa$ did not bind to the recombination signal sequences but instead bound to sites in the EBV C-promoter and in the CD23 promoter.

Epstein-Barr virus infects human B lymphocytes and epithelial cells and immortalizes B cells. In these cells, the EBV genome establishes latency and is stably maintained in the nucleus as an episome in which only a subset of the viral genome (about 10 genes) is expressed (*1, 2*). A virally encoded transcription factor, EBNA2, is required for both B cell immortalization and the establishment of latency (*3, 4*). EBNA2 transactivates latent viral genes and certain cellular genes that have been implicated in B cell activation (*5–10*). EBNA2 activates gene expression through a common cis-regulatory element found in both viral and cellular promoters (*11*), yet EBNA2 is unable to bind directly to these regulatory elements. In order to associate with target genes, EBNA2 requires a DNA binding protein encoded by the host cell. This

T. Henkel and M. G. Peterson, Tularik Inc., 270 East Grand Avenue, South San Francisco, CA 94080, USA. P. D. Ling and S. D. Hayward, Molecular Virology Laboratories, Department of Pharmacology and Molecular Sciences and Department of Oncology, The Johns Hopkins University, School of Medicine, Baltimore, MD 21205, USA.

*To whom correspondence should be addressed.

protein, first characterized as a B cell factor binding to the EBV C-promoter (*11*), is CBF1. Because CBF1 is required for EBNA2 binding to viral promoters and to the promoters of B cell activation genes, we purified the protein in order to study its mechanism of action.

Although CBF1 was initially isolated from B cells (*11*), for purification purposes we investigated whether HeLa cells might contain the activity required for EBNA2 transactivation. To analyze the ability of EBNA2 to transactivate gene expression in HeLa cells, we used a hybrid regulatory construct containing eight tandem repeats of the CBF1 binding site from the EBV C-promoter, fused upstream of the adenovirus E1b TATA box (*12*). This construct specified substantial amounts of reporter protein [chloramphenicol acetyltransferase (CAT)] activity only when cotransfected with an EBNA2 expression vector (Fig. 1A). As previously described, an EBNA2 mutant (*11*) (EBNA2WW, containing two amino acid substitutions, WW to SR at amino acids 323 and 324) failed to activate the reporter construct (*13*). A reporter construct lacking the CBF1 binding sites was not activated by EBNA2. Gel mobility shift assays comparing extracts from B cells and HeLa cells confirmed that the latter contain a C-promoter binding activity similar to that of CBF1 (Fig. 1B). The HeLa cell bandshift is supershifted by native EBNA2 but not by the EBNA2WW mutant. Thus, HeLa cells contain an EBNA2-mediating activity that is functionally indistinguishable from that of B cell CBF1.

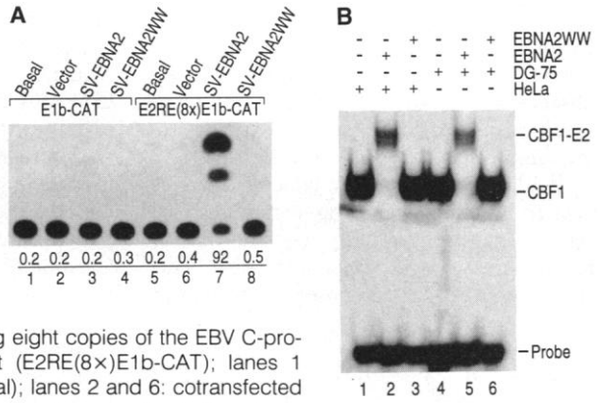

Fig. 1. Transactivation by EBNA2 occurred in HeLa cells and was mediated by CBF1. (**A**) CAT assays in transfected HeLa cells demonstrated that wild-type EBNA2 (SV-EBNA2), but not a mutant EBNA2 (SV-EBNA2WW), transactivates a reporter construct containing EBNA2-responsive elements. Lanes 1 to 4: CAT reporter plasmid lacking EBNA2-responsive elements (E1b-CAT); lanes 5 to 8: CAT reporter plasmid containing eight copies of the EBV C-promoter EBNA2-responsive element (E2RE(8×)E1b-CAT); lanes 1 and 5: nothing cotransfected (basal); lanes 2 and 6: cotransfected with SV40 promoter vector control (vector); lanes 3 and 7: cotransfected with SV40 promoter driving EBNA2 (SV-EBNA2); lanes 4 and 8: cotransfected with SV40 promoter driving a nonfunctional EBNA2 containing the WW323SR double point mutation (SV-EBNA2WW). The percentage conversion of [^{14}C]chloramphenicol is indicated below each lane. HeLa cells were transfected (*22*) with plasmid constructs (*12*), and CAT assays were done as described (*12*). (**B**) Electrophoretic mobility-shift assay (EMSA) comparing CBF1 derived from B cells and from HeLa cells. Nuclear extracts were added to DNA binding reactions with a ^{32}P-labeled probe containing the C-promoter EBNA2-responsive element (Cp) (*12*) and the same amount of unlabeled Cp-mutant oligonucleotide (Cp-mut). The sequences of the Cp and Cp-mut oligonucleotides are shown in Fig. 4. Lanes 1 to 3: HeLa nuclear extracts; lanes 4 to 6: B cell–line DG-75 nuclear extracts; lanes 2 and 5: nuclear extracts with added GST-EBNA2 (EBNA2 amino acid residues 252 to 425 fused to GST) (EBNA2); lanes 3 and 6: nuclear extracts with added GST-EBNA2WW (EBNA2 amino acid residues 252 to 425 containing the WW323SR double point mutation fused to GST) (EBNA2WW). The ^{32}P-labeled probe (probe), CBF1-probe (CBF1), and CBF1-EBNA2-probe (CBF1-E2) complexes are indicated. Nuclear extracts (*23*), GST-fusion proteins, and EMSA conditions were as described (*11*).

CBF1 was purified from HeLa cells with heparin-Sepharose chromatography, followed by DNA-affinity chromatography with the C-promoter binding site (Fig. 2A). Pure CBF1 consisted of a 60-kD polypeptide and a minor polypeptide that migrated slightly more slowly when run on denaturing polyacrylamide gels (Fig. 2B). Both of these polypeptides co-purified with CBF1 binding activity when determined by bandshift analysis with a C-promoter recognition site and by supershift analysis with EBNA2. Purified CBF1 was digested with trypsin, and the resulting peptides were purified by reversed-phase high-pressure liquid chromatography. The peptide sequences (Fig. 2C) showed that CBF1 is identical to a previously characterized protein, the recombination signal–binding protein of J_κ (RBPJ_κ) (*14*, *15*).

To test whether RBPJ_κ has CBF1 activity (DNA-binding and EBNA2-interaction activity), we cloned the complementary

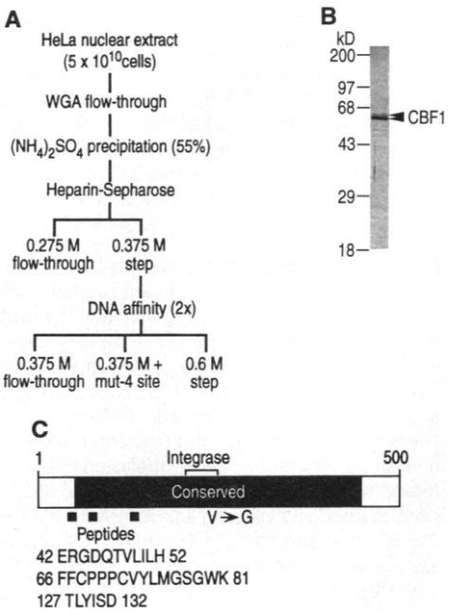

Fig. 2. Identification of CBF1 as the recombination signal–binding protein of J_κ (RBPJ_κ). (**A**) Purification scheme for CBF1. HeLa cells (5 × 10^{10}) were extracted (*24*) and chromatographed on wheat germ agglutinin (WGA) as described (*25*). The CBF1 activity was precipitated from the WGA flow-through by the addition of ammonium sulfate to 55%. The pellet was resuspended in and dialyzed into 0.275 M KCl in HEG buffer [25 mM Hepes (pH 7.9), 0.5 mM EDTA, 20% glycerol, 1 mM dithiothreitol, 0.1% aminoethylbenzenesulfonyl fluoride, 0.1% sodium metabisulfite, and 0.05% lauryldimethylamineoxide] and then applied to heparin-Sepharose (5 mg/ml) equilibrated in the same buffer. CBF1 activity was step-eluted with 0.375 M KCl in HEG buffer, poly(dI-dC) (25 μg/ml) was added, and the solution was applied directly to a DNA-affinity column equilibrated in the same buffer. The DNA-affinity resin consisted of a double-stranded C-promoter EBNA2-responsive element (dGGAAACACGCCGTGGGAAAAAATTTGGG) bound by means of a 5′ end biotin on the sense strand to avidin-agarose (0.5 mg oligo per milliliter of avidin-agarose). Bound proteins were washed with two column volumes of 0.375 M KCl in HEG buffer containing 500 μg/ml double-stranded C-promoter EBNA2-responsive element containing a double point mutation (dGGAAACACGCCGTGG*CT*AAAAATTTGGG). CBF1 activity was step-eluted with 0.6 M KCl in HEG buffer. DNA-affinity chromatography was repeated without protease inhibitors. (**B**) Silver-stained SDS-polyacrylamide gel of DNA affinity–purified CBF1 from HeLa cells. A doublet at approximately 60 kD is indicated as CBF1. (**C**) Schematic diagram of human CBF1-RBPJ_κ (*13*). The 500–amino acid open reading frame (*15*) contains a conserved region (filled box, 82% identity with *Drosophila*) from amino acids 50 to 454. Within this region is a sequence motif showing some similarity with bacterial integrases (integrase). A single difference between the RBPJ_κ sequence (*15*) and ours [determined on six independent polymerase chain reaction (PCR) products] at amino acid 240 is indicated (V to G). A glycine is found at this position in both the mouse and *Drosophila* sequences. The positions and sequences of the three tryptic peptides obtained from purified CBF1 are shown (peptides). The PCR primers used to amplify the cDNA coding for the 500–amino acid open reading frame of RBPJ_κ from a HeLa cDNA library were: sense strand, dGATATCTAGAGCGCTCCCCATGGACC; antisense strand, dCTAGGGATCCTAGGATACCACTGTGGCTGT.

DNA (cDNA) encoding $RBPJ_\kappa$ from a HeLa cDNA library and expressed the 500–amino acid coding region (Fig. 2C) in human 293 cells and in reticulocyte lysate. Although 293 cells contain endogenous CBF1, the transient expression of $RBPJ_\kappa$ under the control of the strong cytomegalovirus (CMV) promoter resulted in an increased amount of CBF1 binding activity (Fig. 3A). Likewise, reticulocyte lysates programmed with $RBPJ_\kappa$ mRNA yielded a bandshift on the C-promoter site that comigrates with that produced by CBF1. These $RBPJ_\kappa$ bandshift activities functioned like those of purified CBF1 in their ability to form an EBNA2 supershifted complex (Fig. 3A). These data indicate that CBF1 and $RBPJ_\kappa$ are the same protein.

CBF1 and EBNA2 have been interpreted to interact directly in the complex formed on EBNA2-responsive genes (*11*). Because EBNA2 is incapable of binding to the C-promoter site (*16*), we reasoned that EBNA2 might be tethered to target genes by means of direct protein-protein interactions with CBF1. If so, CBF1 and EBNA2 might be capable of interacting in solution. To test this hypothesis, we translated CBF1 in the presence of ^{35}S-labeled methionine (Fig. 3B) and then assayed for specific binding to affinity resins containing various glutathione-S-transferase (GST) fusion proteins. Radiolabeled CBF1 bound to GST-EBNA2 but not to GST-EBNA2WW (the mutant that was unable to supershift the CBF1-DNA complex and failed to activate the C-promoter reporter construct) nor to two other protein controls. These observations indicate that CBF1 interacts specifically with EBNA2 and that this interaction can occur in the absence of DNA.

$RBPJ_\kappa$ was originally characterized as a protein that binds to the recombination signal sequence of the J_κ segment that is required for V(D)J recombination (*14*). The signal sequence is composed of heptamer (CACTGTG) and nonamer (GGTTTTTGT) motifs separated by a nonconserved spacer. $RBPJ_\kappa$ was found by bandshift and footprint analysis to bind to the heptamer sequence (*17*) and was thought to be involved in immunoglobulin gene recombination. The heptamer sequence, however, bears little resemblance to the conserved core of the EBNA2 responsive element (GTGGGAAA) that is critical for CBF1 binding (*16*). On inspection of the DNA probes that were used for the $RBPJ_\kappa$ experiments, we noticed that the heptamer site was positioned adjacent to a Bam HI linker sequence and created the sequence GTGGGA—a sequence that is a close match to the CBF1 consensus sequence.

To investigate whether this artificial site is capable of binding CBF1, we tested the various potential CBF1 binding sites as competitors in a bandshift assay, using the C-promoter site as a probe. To set the range for competitor sites, we first compared a mutant that is severely defective in CBF1 binding with the native C-promoter site that contains a consensus EBNA2 response element. The mutated binding site (Cp-mut) was approximately 250 times weaker as a competitor than was the optimal C-promoter site (Cp) (Fig. 4). An EBNA2-responsive element derived from the CD23 promoter (CD23p) was only slightly weaker (~2.5 times) than the C-promoter site. The J_κ heptamer and the adjacent Bam HI site (heptamer + Bam HI) were approximately 16 times weaker than the C-promoter site in this competition assay. Mutation of the GGA residues of the Bam HI site to CCT (heptamer − Bam HI), which left the conserved heptamer sequence intact, reduced the fragment's ability to compete for CBF1 binding to one-fortieth of its previous value. We therefore conclude that CBF1 does not bind the J_κ heptamer sequence to any substantial extent (*18*). Because the name $RBPJ_\kappa$ is misleading, we will refer to this protein as CBF1.

Considerable information has already emerged regarding the structure, expression, and conservation of CBF1. The amino acid sequence of CBF1 is evolutionarily conserved between species as divergent as human and *Drosophila* (Fig. 2C) (*19, 20*). Studies of the tissue distribution of mouse CBF1 show that the mRNA and the protein are expressed in all tissues analyzed (*21*). In *Drosophila*, the CBF1 homolog is encoded by the *suppressor of hairless* gene (*19, 20*). Thus, although CBF1 appears to be quite widely expressed during *Drosophila* development, it plays a key role in the specification of neuronal cell fate.

EBNA2 activates a number of B cell activation genes such as CD21 and CD23, both of which contain CBF1 sites. In the resting B cell that EBV infects, these genes are ex-

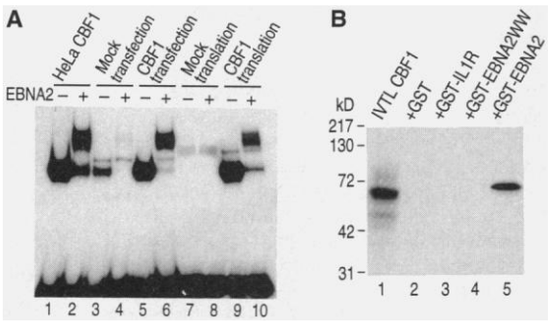

Fig. 3. DNA binding and EBNA2 interaction of recombinant CBF1. (**A**) Electrophoretic mobility-shift assay of transfected and in vitro–translated recombinant CBF1. Lanes 1 and 2: purified CBF1 from HeLa cells (HeLa CBF1); lanes 3 and 4: nuclear extract from mock-transfected 293 cells (Mock transfection); lanes 5 and 6: nuclear extract from 293 cells transfected with CMV promoter driving CBF1 (CBF1 transfection); lanes 7 and 8: reticulocyte lysate programmed with irrelevant mRNA (Mock translation); lanes 9 and 10: reticulocyte lysate programmed with CBF1 mRNA (CBF1 translation); lanes 2, 4, 6, 8, and 10: GST-EBNA2 (EBNA2 amino acid residues 252 to 425 fused to GST) added (EBNA2). Transient transfections (*22*), GST-EBNA2 fusion, and EMSA conditions were as described (*11*). (**B**) SDS–polyacrylamide gel electrophoresis showing the interaction of EBNA2 with ^{35}S-labeled in vitro–translated CBF1. Lane 1: in vitro–translated CBF1 (IVTL CBF1); lane 2: in vitro–translated CBF1 affinity purified on GST beads (+GST); lane 3: in vitro–translated CBF1 affinity purified on GST–interleukin-1 receptor beads (+GST-IL1R); lane 4: in vitro–translated CBF1 affinity-purified on GST-EBNA2 (EBNA2 amino acid residues 252 to 425 containing the WW323SR double point mutation fused to GST) (+GST-EBNA2WW); lane 5: in vitro–translated CBF1 affinity-purified on GST-EBNA2 (EBNA2 amino acid residues 252 to 425 fused to GST) (+GST-EBNA2). Aliquots (7.5 μl) of CBF1 in vitro translation were mixed with equal amounts of GST fusion proteins. Glutathione-agarose beads were added and complexes were formed in 1 ml of phosphate-buffered saline and 0.5% NP-40 for 1 hour at 4°C. Complexes were washed with 5 × 1 ml of phosphate-buffered saline and 0.5% NP-40.

CBF1 binding-site competitor DNA		Reduction (%)		
		Pmol Competitor		
		0.1	1.0	10
Cp	GGAAACACGCCGTGGGAAAAAATTTGGC CCTTTGTGCGGCACCCTTTTTTAAACCG	51	90	98
Cp-mut	GGAAACACGCCGTGGCTAAAAATTTGGG CCTTTGTGCGGCACCGATTTTTAAACCC	0	0	19
CD23p	TCCTTCAGCCCTGTGGGAACTTGCTGCT AGGAAGTCGGGACACCCTTGAACGACGA	22	70	91
Heptamer + Bam HI	GGACTACCACTGTGGGATCCTCTGGAGG CCTGATGGTGACACCCTAGGAGACCTCC	0	31	75
Heptamer - Bam HI	GGACTACCACTGTGCCTTCCTCTGGAGG CCTGATGGTGACACGGAAGGAGACCTCC	0	0	8

Fig. 4. Binding of purified CBF1 from HeLa cells to naturally occurring and mutant promoter elements. Double-stranded oligonucleotides were derived from: EBV C-promoter (Cp), EBV C-promoter containing a double point mutation (Cp-mut), human CD23 promoter (CD23p), heptamer site from human J_κ segment + Bam HI site (Heptamer + Bam HI), and heptamer site from human J_κ segment + Bam HI site containing a triple point mutation (heptamer − Bam HI). The consensus CBF1 binding site is in bold and the J_κ heptamer sequence is underlined. Binding is expressed as the percentage of inhibition of a CBF1 bandshift with 0.1 pmol of ^{32}P-labeled Cp-oligonucleotide, as measured with the indicated amount of competitor oligonucleotide. The EMSA conditions were as described (*11*); the intensities of the bandshifts were determined with a phosphoimager.

pressed at a low level. In the simplest model, CBF1 acts to tether EBNA2 to the promoters of otherwise quiescent target genes. Because EBNA2 contains a transcriptional activation domain (*12*), the promoter-bound protein could act locally to induce transcription in a manner similar to that of conventional transcription factors. By using CBF1 as a target for EBNA2, EBV effectively subverts the ability of B cells to control the expression of these genes. Moreover, EBNA2 might mimic a cellular factor that normally binds CBF1 and activates B cell genes in response to stimuli. This interpretation offers a new focal point for future studies concerning B cell activation.

REFERENCES AND NOTES

1. E. Kieff and D. Liebowitz, in *Virology*, B. N. Fields and D. M. Knipe, Eds. (Raven, New York, 1990), pp. 1889–1920.
2. G. Miller, *ibid.*, pp. 1921–1958.
3. J. I. Cohen, F. Wang, J. Mannick, E. Kieff, *Proc. Natl. Acad. Sci. U.S.A.* **86**, 9558 (1989).
4. W. Hammerschmidt and B. Sugden, *Nature* **340**, 393 (1989).
5. M. Cordier *et al.*, *J. Virol.* **64**, 1002 (1990).
6. R. Fahraeus, A. Jansson, A. Ricksten, A. Sjoblom, L. Rymo, *Proc. Natl. Acad. Sci. U.S.A.* **87**, 7390 (1990).
7. X. W. Jin and S. H. Speck, *J. Virol.* **66**, 2846 (1992).
8. N. S. Sung, S. Kenney, D. Gutsch, J. S. Pagano, *ibid.* **65**, 2164 (1991).
9. F. Wang, H. Kikutani, S. F. Tsang, T. Kishimoto, E. Kieff, *ibid.*, p. 4101.
10. U. Zimber-Strobl *et al.*, *EMBO J.* **12**, 167 (1993).
11. P. D. Ling, D. R. Rawlins, S. D. Hayward, *Proc. Natl. Acad. Sci. U.S.A.* **90**, 9237 (1993).
12. P. D. Ling, J. J. Ryon, S. D. Hayward, *J. Virol.* **67**, 2990 (1993).
13. Abbreviations for the amino acid residues are as follows: C, Cys; D, Asp; E, Glu; F, Phe; G, Gly; H, His; I, Ile; K, Lys; L, Leu; M, Met; P, Pro; Q, Gln; R, Arg; S, Ser; T, Thr; V, Val; W, Trp; and Y, Tyr.
14. N. Matsunami *et al.*, *Nature* **342**, 934 (1989).
15. R. Amakawa *et al.*, *Genomics* **17**, 306 (1993).
16. T. Henkel, P. D. Ling, S. D. Hayward, M. G. Peterson, unpublished data.
17. Y. Hamaguchi, N. Matsunami, Y. Yamamoto, T. Honjo, *Nucleic Acids Res.* **17**, 9015 (1989).
18. Since submission of this manuscript, T. Tun *et al.* [*ibid.* **22**, 965 (1994)] have described CGTGGGAA as the consensus binding site for $RBPJ_{\kappa}$, which is in accordance with our data.
19. F. Schweisguth and J. W. Posakony, *Cell* **69**, 1199 (1992).
20. T. Furukawa, S. Maruyama, M. Kawaichi, T. Honjo, *ibid.*, p. 1191.
21. Y. Hamaguchi *et al.*, *J. Biochem.* **112**, 314 (1992).
22. P. M. Lieberman, J. M. Hardwick, S. D. Hayward, *J. Virol.* **63**, 3040 (1989).
23. E. Schreiber, P. Matthias, M. M. Muller, W. Schaffner, *Nucleic Acids Res.* **17**, 6419 (1989).
24. J. D. Dignam, R. M. Lebovitz, R. G. Roeder, *ibid.* **11**, 1475 (1983).
25. S. P. Jackson and R. Tjian, *Proc. Natl. Acad. Sci. U.S.A.* **86**, 1781 (1989).

26. We are indebted to M. Brasseur for his expertise in peptide separation. We thank S. L. McKnight, K. LaMarco, V. Baichwal, D. Goeddel, and D. Kemp for their critical reading of the manuscript. T.H. was the recipient of a fellowship from the Deutsche Forschungsgemeinschaft. Supported by grants to S.D.H. from NIH (CA42245) and the American Chemical Society (FRA429) and by Tularik Inc.

17 March 1994; accepted 9 May 1994

Magnetoreception in Honeybees

Chin-Yuan Hsu and Chia-Wei Li*

Magnetoreception by honeybees (*Apis mellifera*) is demonstrated by such activities as comb building and homing orientation, which are affected by the geomagnetic field. In other magnetoreceptive species, iron oxide crystals in the form of magnetite have been shown to be necessary for primary detection of magnetic fields. Here it is shown that trophocytes, which are apparently the only iron granule–containing cells in honeybees, contain superparamagnetic magnetite. These cells are innervated by the nervous system, which suggests that trophocytes might be primarily responsible for magnetoreception. Electron microscopy also shows cytoskeletal attachments to the iron granule membrane.

The magnetic field of the Earth influences the behavior and orientation of a variety of organisms, such as magnetotactic bacteria (*1*), algae (*2*), marine mollusks (*3*), honeybees (*4*), hornets (*5*), salmon (*6*), tuna (*7*), turtles (*8*), salamanders (*9*), homing pigeons (*10*), cetaceans (*11*), and human beings (*12*). One of the best understood examples of magnetoreception and magnetonavigation is that of magnetotactic bacteria, whose magnetoreceptors are single-domain particles of magnetite (Fe_3O_4), arranged in a chain along the long axis of each bacterium (*13*). These bacteria swim to the north in the Northern Hemisphere, to the south in the Southern Hemisphere, and in both directions at the geomagnetic equator (*14*). In metazoans, the precise localization of single-domain magnetites and the linkage of these crystals to functioning sensory nerves that transmit magnetic field information to the central nervous system have not been determined, even though single-domain magnetite particles have been extracted from the dermethmoid tissue of the yellowfin tuna (*15*), the forehead of salmon (*16, 17*), the dura mater of green turtles (*8*), and from human brain tissue (*18*).

The existence of a magnetoreceptor in honeybees has been suggested by behavioral and biochemical studies. Worker bees are magnetic (*19*), as measured by superconducing quantum interference devices, and magnetite has been obtained from the abdomens of dried bees, as shown by the abdomen tissue's Curie temperature and magnetization. In honeybees, the only cells that contain iron granules are the trophocytes, which surround each abdominal segment (*20*). Iron deposition in the trophocytes begins on the second day after eclosion, and the iron granule is subsequently formed by the aggregation of dense particles (approximately 7.5 nm in diameter) in the iron deposition vesicles (*21*). However, the iron granules have seemed not to be crystals (*20, 21*) and thus would not be expected to contribute to the measured permanent magnetism. This discrepancy has been accounted for by the low concentration of magnetite in situ—a few parts per billion (*22*).

We determined the presence and nature of the magnetite in honeybee trophocytes by examining the fine structure of the iron granules in the trophocytes with high-resolution transmission electron microscopy (HRTEM). Adult worker bees, 25 to 35 days after eclosion, were dissected, fixed, and embedded according to the conventional procedure (*21*). Thin sections were cut with a diamond knife and stained with uranyl acetate and lead citrate (*21*). Forty iron granules (Fig. 1A) (from five bees) with an average diameter of 0.6 μm were analyzed by a JEOL 4000EX HRTEM operating at 400 kV. Crystals were found in the central portion of four of the examined iron granules. The crystallized central portion occupied 30% of the granule volume. The largest crystal was approximately 10 nm in diameter. The direction of lattice structure in nearby crystals was random, and the lattice fringes often appeared to extend across the region of 7.5-nm electron-dense particles (Fig. 1B). A diffraction pattern (Fig. 1D) was obtained from a lattice image (Fig. 1C) by Fourier transformation. The *d*-spacings calculated from the diffraction pattern were consistent with the [1 $\bar{2}$ 1] zone axis pattern of magnetite (*23*). All of the magnetite crystals showed well-ordered lattice planes, and none of the crystals had any other crystalline phases, such as those typical of γ-FeOOH. Previous investigators may not have obtained diffraction patterns from these crystals because of the crystals' small size.

If the observed superparamagnetic granules are indeed the honeybees' magnetoreceptors, then nervous system innervation of the trophocytes would be expected. The abdominal areas of adult worker bees, 25 to

C.-Y. Hsu, Institute of Life Science, National Tsing Hua University, Hsinchu, Taiwan, Republic of China.
C.-W. Li, Institute of Life Science, National Tsing Hua University, Hsinchu, and National Museum of Natural Science, Taichung, Taiwan, Republic of China.

*To whom correspondence should be addressed at National Tsing Hua University.